Pergamon

Int. J. Heat Mass Transfer. Vol. 38, No. 5, pp. 807–818, 1995

0017–9310/95 $9.50+0.00

0017–9310(94)00208–8

Predictive and diagnostic aspects of a universal thermodynamic model for chillers

J. M. GORDON† and KIM CHOON NG

Department of Mechanical and Production Engineering, National University of Singapore, 10 Kent Ridge Crescent, Singapore 0511

(*First received* 10 *May* 1994 *and in final form* 7 *July* 1994)

Abstract—There are fundamental aspects of chiller behavior—characterized by the chiller coefficient of performance as a function of cooling rate and coolant temperatures—that pertain to all refrigeration devices. We review, further develop, and validate against extensive experimental measurements a simple thermodynamic model that captures the universal aspects of chiller behavior. The model provides a procedure for predicting chiller performance over a broad range of operating conditions from a small number of selected measurements, as well as a diagnostic tool. The accuracy of the model is illustrated for reciprocating, centrifugal and absorption chillers. Universal aspects of chiller behavior are further illustrated with less conventional small-scale cooling devices such as thermoacoustic and thermoelectric chillers.

1. INTRODUCTION

1.1. *Motivation and background*

Are there universal elements in the thermodynamic performance of all chillers—elements from which accurate predictive and diagnostic modeling tools can be developed? If so, to what degree would a model based on these common elements be valid for refrigeration devices as diverse as reciprocating, absorption and thermoelectric chillers? The purpose of this paper is to review, and to develop further, a thermodynamic model that pertains to all chillers, and is simple enough to yield analytic formulae for chiller performance characteristics. One needs to capture the essential physics of the problem by subsuming the dominant contributions to the irreversibilities in chiller operation, while showing how the model can be adapted to the specific loss mechanisms inherent to each chiller type. The predictive and diagnostic value of the model developed here will be compared against actual experimental performance data.

By the rubric 'chillers', we refer to all cooling and refrigeration devices, independent of coolant or application. The vast majority of commercial units are reciprocating and centrifugal chillers, shown schematically in Fig. 1(a). In a relatively small but growing number of large installations, absorption chillers can provide attractive alternatives [shown schematically in Fig. 1(b)]. Low-power, isolated cooling needs are sometimes met with less conventional chiller types, such as thermoelectric and thermoacoustic refrigerators [see Fig. 1(c) and (d)].

Aside from the reversible (Carnot) limit for the chiller coefficient of performance (COP) in terms of effective heat reservoir temperatures, no model has been proposed that pertains to *all* chiller types, covers the full range of operational cooling capacities, and provides accurate predictions of chiller performance. COP is defined as the ratio of the chiller cooling capacity to the power input, where the power input is usually electrical, but can be thermal, acoustic, magnetic or otherwise. Thermodynamic models of chillers are invariably case-specific, being tailored to particular components and operating modes. This means that, when accurate performance predictions are required over a wide range of cooling rates, many experiments must be performed, and extrapolation beyond the measured range may not be valid. This is evidenced by the performance data and associated caveats published in manufacturers' catalogs [1–5]. It also means that diagnostic capabilities based upon a modest number of measurements are severely limited.

In this article, we examine a relatively simple, universal thermodynamic model for chillers—a model that is easily adapted to different kinds of chillers. The model affords accurate predictions of chiller performance over a broad span of operating conditions from a handful of measurements, and can be used for rapid diagnostics. In addition, in capturing the basic physics of the irreversibilities that govern chiller behavior, the model provides a common framework for understanding and comparing the fundamental performance characteristics of all chillers. The examples we present in support of these claims are reciprocating, centrifugal, absorption, thermoelectric and thermoacoustic chillers. In principle other chillers

†On sabbatical leave from: Center for Energy and Environmental Physics, Jacob Blaustein Institute for Desert Research, Ben-Gurion University of the Negev, Sede Boqer Campus 84993, Israel, and the Pearlstone Center for Aeronautical Engineering Studies, Department of Mechanical Engineering, Ben-Gurion University of the Negev, Beersheva, Israel.

NOMENCLATURE

A_0, A_1, A_2, A_3, A_4 constants in equations (8) and (9) for reciprocating chillers
B_1, B_2 constants in equation (15) for absorption chillers
C coolant specific heat
COP coefficient of performance, (cooling rate)/(power input)
h_X factor in equation (6) that depends on heat exchanger properties only
I electrical current
K thermal conductance of thermoelectric
m coolant mass flow rate
n parameter in empirical fit [equation (11)]
NTU number of transfer units of heat exchanger, $UA/(mC)$
P_{in} power input
q_a rate of losses at the absorber of an absorption chiller
q_c rate of losses at the condenser
q_e rate of losses at the evaporator
q_g rate of losses at the generator of an absorption chiller
q_r rate of total internal losses in heat rejection from an absorption chiller
Q heat flow rate
Q_a heat rejection rate from the absorber of an absorption chiller
Q_c heat rejection rate (to the hot reservoir)
Q_e cooling capacity (rate of heat withdrawn from the cold reservoir)
Q_g input thermal power to the generator of an absorption chiller
R total electrical resistance of thermoelectric
T temperature
T_c condenser temperature
T_c^{in} condenser coolant inlet temperature
T_{cold} cold-reservoir temperature
T_e evaporator temperature
T_e^{out} evaporator coolant outlet temperature
T_{hot} hot-reservoir temperature
T_o temperature parameter in empirical fit [equation (11)]
T^* parametric chiller temperature, $(A_0+A_2)/A_1$
UA heat exchanger thermal conductance.

Greek symbol
α differential thermoelectric power (differential Seebeck coefficient).

should conform equally well to our analysis. The chiller types we consider represent the overwhelming majority of current large commercial and small specialized refrigeration units. Details of the chiller performance tests which form the basis for the experimental measurements cited in this paper can be found in the standards procedures of the Air Conditioning and Refrigeration Institute [6–8].

1.2. *Characteristic performance curves*

Chillers can be characterized by their curves of 1/COP against 1/(cooling rate) [9]. The qualitative features for real chillers are shown in Fig. 2. COP should increase with cooling rate at *low* cooling rates due to irreversibilities such as fluid friction (sometimes referred to as isentropic losses since adiabatic expansion and compression processes that would ideally occur isentropically actually generate entropy), throttling losses in the expanding device, de-superheating in the condenser, and heat leaks. Losses that stem from finite-rate heat transfer will dominate at *high* cooling rates, so that COP should decrease as cooling rate increases. There should be an intermediate range of cooling capacities in which COP passes through a maximum value.

The specific irreversibilities cited above pertain to conventional large commercial chillers. It appears that, independent of chiller type, there will always be irreversibilities that disfavor very fast and very slow cooling rates. Hence COP will vanish in both these limits.

One should distinguish between how each irreversibility contributes to the magnitude of the chiller COP, and how it affects the COP cooling-rate dependence. For example, the thermal bottleneck of finite-rate heat transfer may comprise a significant fraction of the total COP at all cooling rates, but may contribute negligibly to the dependence of COP on cooling rate at relatively low cooling rates, which is the linear regime in Fig. 2(a). This point is illustrated in Fig. 2(b)—a non-quantitative plot that shows the trends and relative magnitudes of different irreversibilities. In the linear region, where most commercial chillers operate, finite-rate heat exchange may comprise more than half the overall COP, but it contributes insignificantly to the dependence of COP on cooling rate (i.e. to the slope of the curve).

Nearly all reported performance data for commercial chillers fall on the linear part of the characteristic curve in Fig. 2 [1–3, 5, 9]. This observation will be exploited in arriving at a model that, with two or three adjustable parameters, can accurately account for the functional dependence of COP on all key readily-measurable chiller variables. In cases where deviations from such linear behavior are prominent, the qualitative trends in characteristic chiller

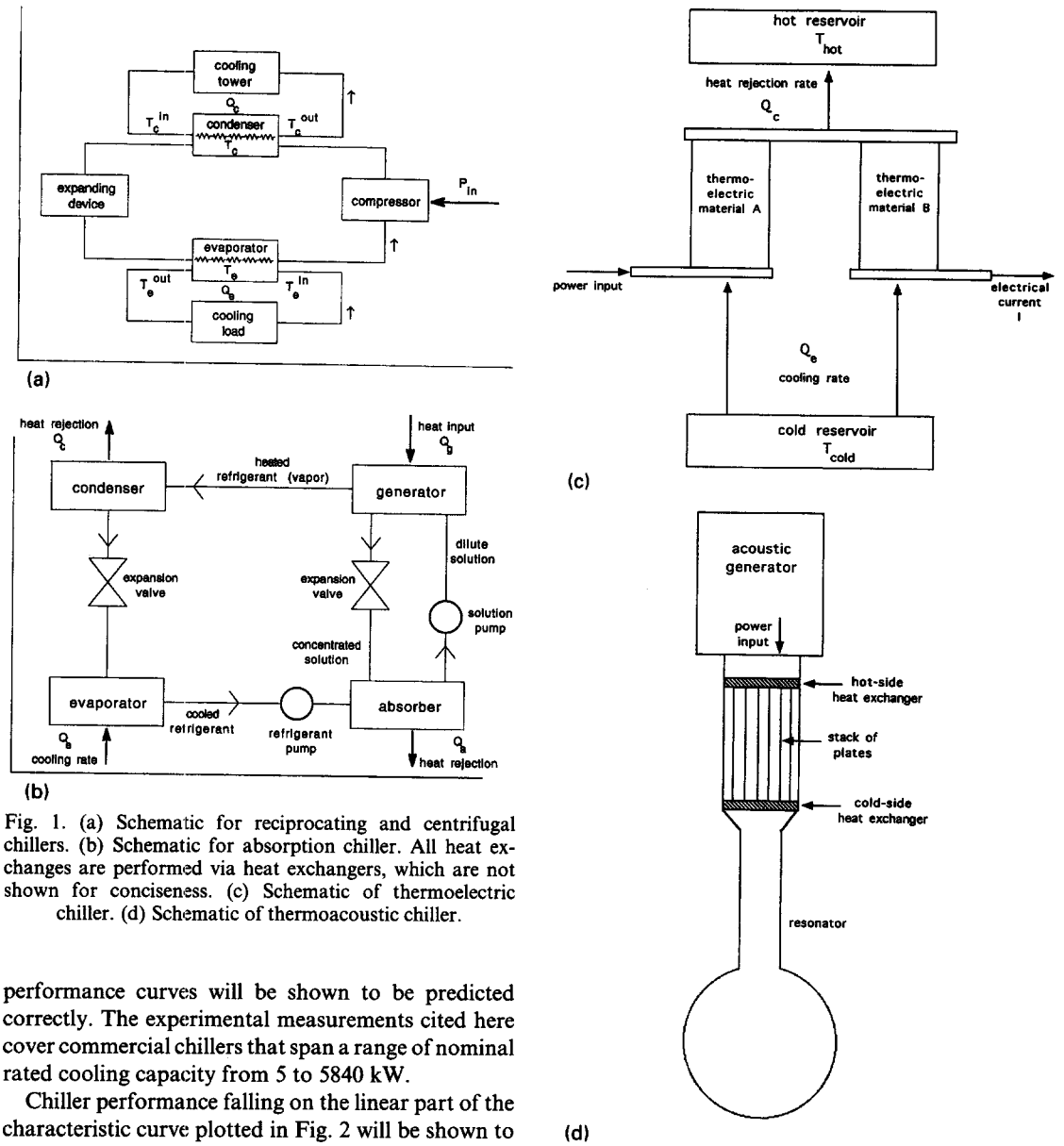

Fig. 1. (a) Schematic for reciprocating and centrifugal chillers. (b) Schematic for absorption chiller. All heat exchanges are performed via heat exchangers, which are not shown for conciseness. (c) Schematic of thermoelectric chiller. (d) Schematic of thermoacoustic chiller.

performance curves will be shown to be predicted correctly. The experimental measurements cited here cover commercial chillers that span a range of nominal rated cooling capacity from 5 to 5840 kW.

Chiller performance falling on the linear part of the characteristic curve plotted in Fig. 2 will be shown to signify that losses that mitigate against high cooling rates, in particular finite-rate heat transfer, depend negligibly on cooling rate, relative to the other irreversibilities. The non-linear regions in Fig. 2 will only be observed at relatively high cooling capacities, which means larger relative contributions to the COP cooling-rate dependence, from losses that militate against fast operation.

First, we review the derivation of the thermodynamic model and the associated prediction of the universal features of the characteristic performance curve of chillers, 1/COP plotted against 1/(cooling capacity). Thereafter, the principal classes of chillers are considered individually in terms of the specific irreversibility mechanisms that dominate their behavior, and how these losses can be modeled analytically. The predictive and diagnostic powers of the model are then tested against experimental performance data for the principal chiller classes.

Fig. 1—*continued.*

2. COMMON ELEMENTS OF THE THERMODYNAMIC MODEL

Consider first the elements of a general thermodynamic model that are common to almost all chillers. Subsequently, we will introduce assumptions that are specific to different chiller types, while still retaining the general framework and analytic approach. We consider cyclic chiller operation at steady state; transients are neglected.

Entropy and internal energy are thermodynamic state functions, so over one cycle the change in these variables for the chiller working fluid is zero. Using the observation that the net change in the internal energy of the chiller working fluid is zero, together with the first law of thermodynamics, yields

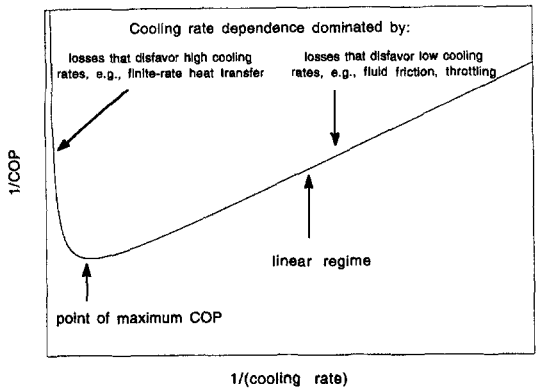

(a)

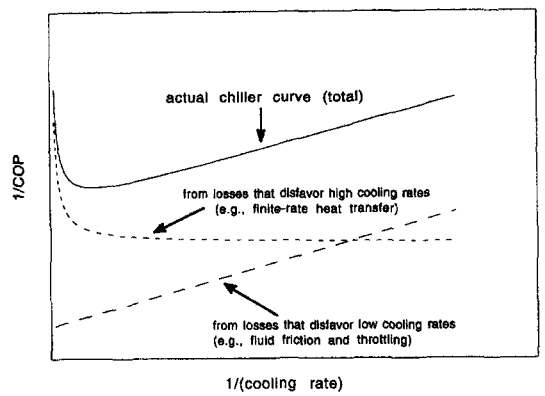

(b)

Fig. 2. (a) Characteristic chiller performance curve. (b) Characteristic chiller curve shown as comprised of separate contributions from losses that disfavor high cooling rates and losses that disfavor low cooling rates (not quantitative).

$$0 = P_{in} - Q_c + Q_e \tag{1}$$

where P_{in} is the power input, Q_e is the cooling capacity (rate of heat withdrawn from the cold reservoir), and Q_c is the heat rejection rate (to the hot reservoir), with all variables referring to cycle-average quantities. All energy flows are defined here as positive. In almost all commercial chillers, the hot side refers to the condenser, and the cold side to the evaporator (hence the subscripts c and e). In the ensuing descriptions, we will employ this nomenclature, although the analysis applies to any refrigeration scheme.

The zero net change in entropy for the chiller working fluid can be expressed as

$$0 = \frac{Q_c + q_c}{T_c} - \frac{Q_e + q_e}{T_e} \tag{2}$$

where T_c and T_e are the temperatures of the condenser and evaporator fluid, respectively, and q_c and q_e denote the rate of losses at the condenser and evaporator sides, respectively, that stem from internal dissipation.

Heat transfer processes have been approximated as isothermal. In reality, they are not isothermal; but one can either view these deviations from isothermal behavior as small relative to the absolute temperatures T_c and T_e, and/or can adopt process-averaged values of T_c and T_e, as is commonly done for effective hot- and cold-side temperatures in heat exchanger analyses [10]. Explicit formulae for q_c and q_e, that depend on the particular kind of chiller and on readily-measured chiller variables, will be derived in the sections that follow.

Defining the chiller COP by

$$\mathrm{COP} = Q_e / P_{in} \tag{3}$$

we combine equations (1)–(3) to obtain

$$1/\mathrm{COP} = -1 + (T_c/T_e) + (1/Q_e)\left[\frac{q_e T_c}{T_e} - q_c\right]. \tag{4}$$

Commercial chillers operate with heat exchangers at the condenser and evaporator ends, and it is the heat exchanger inlet and outlet temperatures, rather than actual condenser and evaporator temperatures, that are commonly (and easily) measured, and reported in manufacturers' catalogs. Heat exchanger inlet and outlet temperatures will be denoted with superscripts 'in' and 'out', respectively. The temperature T of the condenser or evaporator working fluid can be expressed in terms of the fluid inlet temperature on the secondary of the heat exchanger T^{in}, the heat flow Q in W, the mass flow rate m, the coolant specific heat C, and the number of transfer units NTU $[(UA)/(mC)$, with UA denoting the overall thermal conductance of the heat exchanger in W K^{-1}]:

$$T = T^{in} + \frac{Q\{1 - \exp(-\mathrm{NTU})\}}{mC}. \tag{5}$$

This enables us to express COP in terms of T_c^{in} and T_e^{out}:

$$1/\mathrm{COP} = -1 + (T_c^{in}/T_e^{out}) + (q_e h_X T_c^{in}/T_e^{out}) + (1/Q_e)\left[\frac{q_e T_c^{in}}{T_e^{out}} - q_c\right] + \text{terms of order } Q_e \text{ and higher} \tag{6}$$

where h_X is a factor that depends only on the heat exchanger properties noted above. The analysis is simplified considerably by recognizing that the losses that stem from finite-rate heat transfer in commercial chillers are sufficiently small that the higher-order terms in equation (6) turn out to be negligible. Furthermore, heat exchanger NTU values are sufficiently high that the h_X term in equation (6) turns out to be negligible, i.e. $q_e h_X \ll 1$. Hence actual chiller performance appears to lie in a regime of relatively low cooling capacities. Actually, it is simply the relative contribution of finite-rate heat transfer to the COP cooling-rate dependence being small compared to that of other irreversibilities.

There are situations in which the cooling-rate dependence of the dissipation due to finite-rate heat transfer grows noticeable. This contingency is analyzed for reciprocating chillers in Section 3.3. The onset of non-linearities in the chiller characteristic

curve (Fig. 2) can also be observed in manufacturer catalog data for absorption chillers, as shown in Section 5.3, and forms a considerable part of the measurable performance curve for the thermoacoustic and thermoelectric refrigerators, as shown in Sections 6 and 7. For now, we proceed with an analysis that corresponds to most commercial, properly-operating devices, based on actual experimental data, i.e. 1/COP being a linear function of $1/Q_e$.

The approximate derived relation is

$$1/\mathrm{COP} = -1 + (T_e^{in}/T_e^{out}) + (1/Q_e)\left[\frac{q_e T_c^{in}}{T_e^{out}} - q_c\right]. \tag{7}$$

The commonly-measured chiller variables are: Q_e, COP (or, equivalently, P_{in}), T_c^{in} and T_e^{out}. A plot of 1/COP against $1/Q_e$ should be a straight line, the slope of which will depend on the irreversibility mechanisms particular to a given chiller class. As shown in recent studies for reciprocating and absorption chillers [9, 11], this is borne out by actual chiller performance data.

Commercial chillers, and in fact all chillers, exhibit the linear relation of equation (7) at sufficiently low cooling rates. For a small number of commercial chillers, and for certain less conventional refrigeration devices, the performance curves can be measured up to relatively high cooling rates, where the cooling-rate dependence of losses that disfavor high cooling rates becomes large, and the full characteristic curve illustrated in Fig. 2 can be observed. The qualitative trend is predicted by the proposed model when one incorporates equation (5) in equation (4), and does not invoke any further approximation. Predictive and diagnostic modeling of chillers in this regime becomes problematic because the number of adjustable parameters, mainly associated with the heat exchangers, becomes excessive. Therefore no quantitative comparisons are attempted here. Nonetheless, the fact that the trend of the theoretical predictions is substantiated by actual performance data will be documented for several chiller types.

3. RECIPROCATING CHILLERS

3.1. *Specific irreversibilities*

Reciprocating chillers represent the overwhelming majority of chiller installations to date. It has been demonstrated that commercial units operate within the linear region in Fig. 2 [equation (7)] [9]. An accurate predictive model will have to account, then, for the particular functional dependences of the loss terms q_c and q_e, in order to yield a final expression for COP as a function of Q_e, T_c^{in} and T_e^{out} only.

If isentropic, throttling and de-superheating losses are not excessive (typical of those in actual commercial chillers), and, if heat leaks are dominated by a linear heat transfer law, the functional form of the loss terms should be [9, 10]

$$q_c = -A_0 + A_3 T_c \tag{8a}$$

$$q_e = -A_2 + A_4 T_e \tag{8b}$$

where the As are constants. Using equation (8) in equation (7), and defining $A_1 = A_3 + A_4$, one obtains

$$1/\mathrm{COP} = -1 + \frac{T_c^{in}}{T_e^{out}} + \frac{-A_0 + A_1 T_c^{in} - A_2 \dfrac{T_c^{in}}{T_e^{out}}}{Q_e} \tag{9}$$

where the constants A_0, A_1 and A_2 characterize the internal irreversibilities of a particular chiller.

3.2. *Model accuracy*

From a limited number of measurements, one can determine the three parameters A_0, A_1 and A_2 by regression analysis. As a graphical illustration of the method, we show in Fig. 3(a) and (b) the model's accuracy in predicting the basic functional dependences on key system variables for one such representative chiller.

According to equation (9), 1/COP should be a linear function of $1/Q_e$ and two additional independent variables, which can be taken as T_c^{in} and the ratio T_c^{in}/T_e^{out}. A plot of $\{(1/\mathrm{COP}) + 1 - (T_c^{in}/T_e^{out})\}\, Q_e$ against T_c^{in}/T_e^{out} should yield a set of parallel straight lines of slope $-A_2$, each line for a different value of T_c^{in} [see Fig. 3(a)]. This point has been confirmed with experimental performance data from 30 commercial chillers that span cooling capacities from 30 to 1300 kW, and COP values from 2.3 to 6.3 [9].

In a plot of

$$\left(\frac{1}{\mathrm{COP}} + 1 - \frac{T_c^{in}}{T_e^{out}}\right) Q_e + A_2 \frac{T_c^{in}}{T_e^{out}}$$

against T_c^{in}, all data points should collapse to a single straight line with slope A_1 and ordinate-intercept $-A_0$ [see Fig. 3(b)]—a point that was also confirmed in ref. [9].

This procedure was shown to predict measured chiller COP values, over the full range of operating conditions covered in manufacturers' catalogs ($T_e^{out} = 4.4$–15.0°C, and $T_c^{in} = 23.9$–53.0°C), with a root-mean-square (RMS) error of 0.4%, for around 900 data points from 30 reciprocating chillers [see Fig. 3(c)]. The RMS error is markedly less than the experimental uncertainty of $\pm 3\%$ in the measurements reported.

3.3. *Deviations from model linearity*

To see if one can observe the predicted deviations from linearity, we secured performance data for chillers where heat transfer at the heat exchangers is a more significant bottleneck. The temperature differences across each chiller component are then larger, the COPs lower, and the higher-order corrections to the linear approximations exploited in equations (6) and (7) grow in magnitude. This should be manifested in a gradual worsening of the predicted functional dependences in equations (7) and (9), and poorer accuracy of the linear model in predicting the chiller COP. In terms of the general characteristic curve of

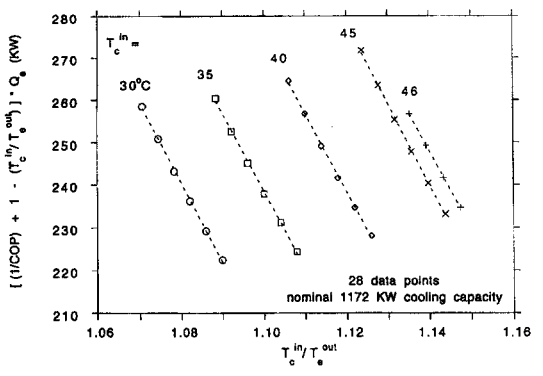

(a)

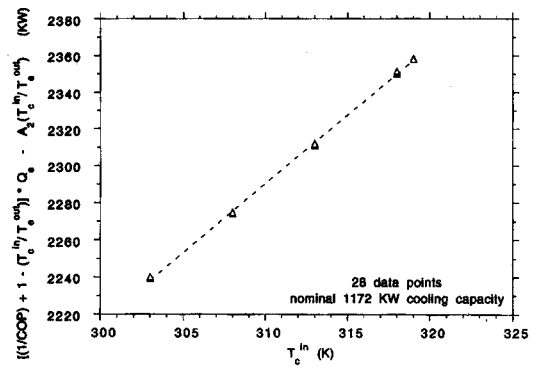

(b)

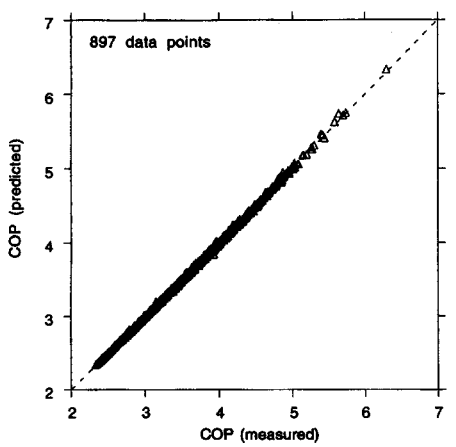

(c)

Fig. 3. (a) Partial check of the predicted functional dependence of equation (9) for a water-cooled reciprocating chiller. The linear model predicts a set of parallel straight lines for different condenser inlet temperatures. (b) A second partial check of the predicted functional dependence of equation (9). Same chiller as for Fig. 3(a). The linear model predicts that all data points should collapse to a single straight line. (c) Illustration of accuracy of linear model in predicting reciprocating chiller COP. Predicted COP is plotted against measured COP for 30 chillers that span nominal cooling capacities from 30 to 1300 kW.

Fig. 2, chiller performance is moving off the linear curve toward a higher cooling capacity.

The manufacturer catalog data we analyzed [4] are for a nominal 63 kW cooling capacity air-cooled chiller, with COPs in the range 1.5–3.5, and cooling capacities of 37–65 kW. Results are presented in Fig. 4. A test of the predicted functional dependence of equation (9) is shown in Fig. 4(a). Unlike Fig. 3(a), there are small but noticeable differences in the slope of each of the straight lines. Furthermore, as shown in Fig. 4(b), all data points do not collapse into a single linear relation, as predicted by equation (9) [contrast with Fig. 3(b)]. Finally, obtaining the best three-parameter fit of equation (9), and summing over all 24 data points [4], we find that the predicted COPs have an RMS error of 4% relative to measured values [see Fig. 4(c), and compare with Fig. 3(c)].

There should be two different ways in which the high cooling capacity, non-linear regime of the characteristic curve in Fig. 2 can be accessed. One is simply to increase cooling capacity. This is not always realistic in most commercial reciprocating chillers due to mechanical and operational constraints. The other way is to examine chillers with a relatively large contribution to the COP cooling-rate dependence from the irreversibility of finite-rate heat transfer. COP then degrades, and what we measure at the same *absolute* cooling rate as higher-efficiency devices becomes a *relatively* high cooling rate for the particular lower-efficiency chiller. The evidence cited above for observable non-linear chiller behavior stems from the latter method.

3.4. *Empirical observations*

A practical and attractive objective is to cast equation (7) or (9) as a universal expression for *all* reciprocating chillers, in terms of non-dimensional variables and coefficients. Such attempts have been made [12] but tend to be restricted to narrow classes of chillers or a small number of devices. Given that the relative contributions of the dominant irreversibilities will be different for different chillers, there is no reason to expect that a single formula, with no adjustable parameters, will offer universally accurate predictions.

However, for the reciprocating chillers considered here and in the studies cited above, all of which employ the same working fluid, Freon R-12, we have noted an intriguing relation among the characteristic parameters in equation (9) [9]. The characteristic parametric temperature $T^* = (A_0+A_2)/A_1$ turns out to be 250 ± 5 K. In terms of T^*, equation (9) can then be expressed as

$$1/\mathrm{COP} = \left[\frac{A_1(T_c^{in}-T^*)}{Q_e}\right]+\left[\frac{T_c^{in}-T_e^{out}}{T_e^{out}}\right]\left[1-\frac{A_2}{Q_e}\right] \tag{10}$$

which, adopting the observed constant value of T^* of 250 K, represents a two-adjustable-parameter model, but with a loss of accuracy in predicting COP of 1–2%. One can continue by searching for a correlation of A_1 and A_2 with chiller rated capacity (cooling rate at prescribed test conditions). The correlations then are weaker, and best fits to the data yield a nominally universal form for equation (9), with no adjustable

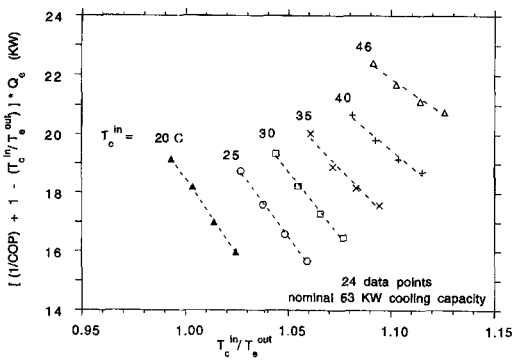

(a)

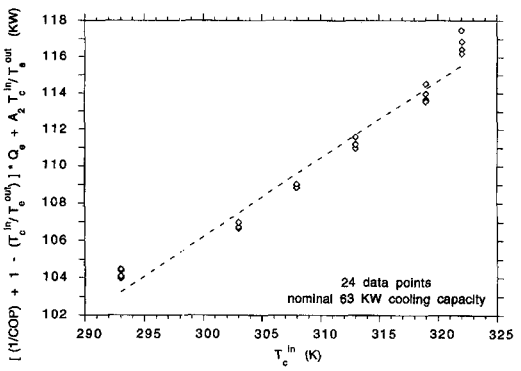

(b)

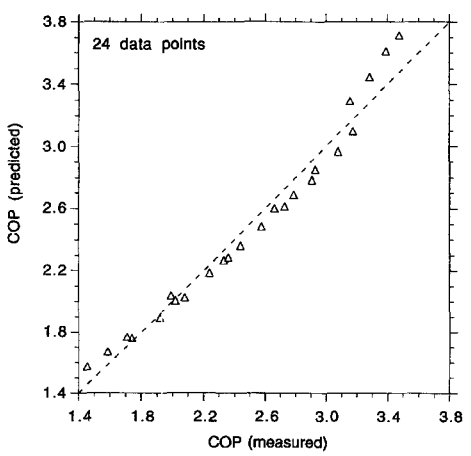

(c)

Fig. 4. (a) Same test for predicted functional dependence as in Fig. 3(a), but for an air-cooled reciprocating chiller where non-linear contributions grow non-negligible. Note that the slopes of the lines change non-negligibly with condenser inlet temperature. This indicates a growing contribution to the dependence of COP on cooling rate from finite-rate heat transfer. (b) Same test for predicted functional dependence as in Fig. 3(b), but for an air-cooled reciprocating chiller where non-linear contributions grow non-negligible. Note the degree to which the measured points do not collapse to a single straight line. This indicates a growing contribution to the dependence of COP on cooling rate from finite-rate heat transfer. (c) Illustration of poorer accuracy of linear model in predicting. COP for the same air-cooled reciprocating chiller as in Fig. 4(a) and (b). Predicted COP is plotted against measured COP.

parameters, but with a significant loss of accuracy in predicting COP.

For a wide range of reciprocating chillers for which manufacturers' catalog data have been published, it was recently noted that, on the RHS of equation (10), the first term is typically about 95% of the total contribution [13]. As a purely empirical, zero-adjustable-parameter formula for these chillers, it was then proposed that performance data be fitted to the expression

$$\mathrm{COP}_{\mathrm{ref}}/\mathrm{COP} = \frac{\left[\dfrac{T_c^{\mathrm{in}} - T_0}{Q_e}\right]^n}{\left[\dfrac{T_c^{\mathrm{in}} - T_0}{Q_e}\right]_{\mathrm{ref}}^n} \tag{11}$$

where the subscript 'ref' refers to chiller variables measured under standard rating reference conditions prescribed in published chiller test procedures [8]. Values of $n = 0.644$ and $T_0 = 268$ K provided the best fit for the chillers investigated.

With over 950 experimental data points from 17 commercial reciprocating chillers that span cooling capacities from 35 to 985 kW, it was demonstrated that equation (11) can reproduce measured COP values with an RMS error of about 1%, which is well within the 5% experimental uncertainty in the measurements. Clearly, equation (11) cannot be valid for all possible chiller operating conditions. It can, however, provide a predictive tool for many of the chillers being installed today, albeit a purely empirical one.

4. CENTRIFUGAL CHILLERS

Whereas our presentation above for reciprocating chillers emphasized the *predictive* power of the thermodynamic model, our analysis for centrifugal chillers will be used to highlight the *diagnostic* value of the model. Centrifugal and reciprocating chillers differ only in their compressors. They may be mechanically and operationally different, but, from the viewpoint of thermodynamic modeling, reciprocating and centrifugal compressors are qualitatively the same, in that the key source of irreversibility is fluid friction losses. Therefore the fundamental linear relation in equation (6) should also be valid for centrifugal chillers.

In this particular diagnostic study, heat exchanger fouling plays a key role. Hence, on the RHS of equation (6), we retain the h_X term. The principal features stressed here are that a plot of $1/\mathrm{COP}$ against $1/Q_e$ should be linear, and that only the (extrapolated) ordinate intercept, and not the slope, should depend on heat exchanger properties.

As described in refs. [14, 15], *in situ* steady-state measurements of an installed centrifugal chiller plant were made over a period of 6 months, in the middle of which chiller maintenance was performed and the heat exchanger tubes were cleaned. Chiller COP had

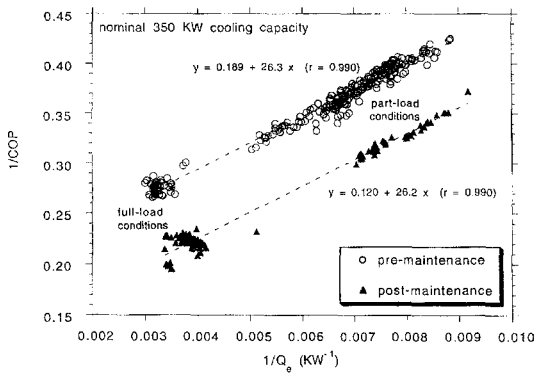

Fig. 5. Characteristic chiller plot for an installed, monitored centrifugal chiller. The upper set of points is for the pre-maintenance monitoring period. The lower set of points is for the post-maintenance period, after the condenser and evaporator heat exchanger tubes were cleaned. Linear regression best fits are indicated. Note expanded axes.

been observed to be undesirably low during the pre-maintenance period. After the heat exchanger tubes were cleaned, chiller COP increased by 36% on average, at roughly the same values of T_c^{in} and T_e^{out}, and at approximately the same values of the cooling rate.

Results based on over 400 steady-state data points, for the pre- and post-maintenance periods, are presented in Fig 5. (The experimental uncertainty in measurements of COP and cooling rate was ± 6.0 and $\pm 4.5\%$, respectively [14].) This type of plot clearly illustrates the natural division into the pre- and post-maintenance periods. The distinction between full- and part-load periods is also evident (the separation of data points, for each period, into high- and low-cooling-rate regimes, respectively).

The plots confirm the predicted linear relation [equation (6)]. The temperature ranges of T_c^{in} and T_e^{out} were sufficiently small that the simple model predicts a single linear relation—one for each monitoring period—with a spread about the average that stems from the fact that T_c^{in} and T_e^{out} did, nonetheless, have some variation. This appears to be confirmed by the experimental measurements. Also, based on values of the extrapolated ordinate-intercept, the h_X term in equation (6) (and hence 1/COP) decreases by 0.07 from the pre- to the post-maintenance period.

The maintenance performed should not have affected the internal irreversibilities of the chiller. Rather, cleaning heat exchanger tubes should only affect the irreversibilities associated with finite-rate heat transfer [the h_X term in equation (6)]. In terms of model predictions, the pre- and post-maintenance periods should exhibit 1/COP vs $1/Q_e$ plots with the same slope but different extrapolated ordinate-intercepts. This is precisely what was observed.

5. ABSORPTION CHILLERS

5.1. *Fundamental aspects of absorption chillers*

Absorption chillers use thermal energy as the driving force, rather than electrical power to run a compressor. The heat input to the generator, usually in the form of gas firing or of the flow of hot water or steam via a heat exchanger, drives part of the volatile component of the solution into the vapor phase, with the reverse process being carried out in the absorber. The condenser and evaporator serve the same functions as in reciprocating chillers.

Absorption chillers also often employ a regenerator between the absorber and the generator, and can be multi-stage (as opposed to single-stage)—steps that improve chiller efficiency for a given heat input. The introduction of these measures does not affect the formulation of the general thermodynamic model developed here, so explicit account of them is not taken. The validity of model predictions pertains equally well to all absorption chillers.

Absorption chillers have the same irreversibilities in the condenser and evaporator as reciprocating and centrifugal chillers. However, performance data from absorption chillers indicate that the dominant irreversibility is finite-rate mass transfer in the generator and absorber [11, 16, 17]. Our model is approximate in the sense of treating losses due to finite-rate mass transfer only, and viewing these losses as temperature-independent. The latter approximation is strengthened by the fact that absorption chillers typically cannot operate over a broad range of generator temperatures [5, 16, 17].

5.2. *Particular irreversibilities*

For absorption chillers, the relation corresponding to the energy balance of equation (1) is

$$0 = Q_g - Q_a - Q_c + Q_e \tag{12}$$

where Q_g is the input thermal power to the generator; and Q_a is the heat rejection rate from the absorber. All energy flows remain defined as positive. COP is defined as Q_e/Q_g. A manufacturer's catalog data usually report Q_e and COP (or, equivalently, Q_g) at assorted values of T_c^{in}, T_e^{out}, T_a^{in} and T_g^{in}.

With heat delivery and rejection performed across heat exchangers, for each of the four major components of the chiller—generator, absorber, condenser and evaporator—the actual temperature in a particular component's working fluid can be expressed as in equation (5). The relation corresponding to the entropy balance of equation (2) is

$$0 = \frac{Q_c - q_c}{T_c} + \frac{Q_a - q_a}{T_a} - \frac{Q_g - q_g}{T_g} - \frac{Q_e - q_e}{T_e} \tag{13}$$

where the q terms refer to losses from all sources other than finite-rate heat transfer.

The validity of equation (7) can be established for most of the operating range of absorption chillers from actual performance data [11]. Denote the total of the irreversible losses associated with heat rejection, $q_c + q_a$, by q_r. Then we obtain the approximate result:

$$1/\mathrm{COP} = \left[\frac{T_c^{in} - T_e^{out}}{T_e^{out}}\right]\left[\frac{T_g^{in}}{T_g^{in} - T_c^{in}}\right] + \left[\frac{1}{Q_e}\right]\left[\frac{T_g^{in}}{T_g^{in} - T_e^{in}}\right]\left[q_r - \frac{T_c^{in}}{T_e^{out}}q_e - \frac{T_c^{in}}{T_g^{in}}q_g\right]. \quad (14)$$

Now we invoke the additional approximation that the dominant irreversibility is finite-rate mass transfer, and that it is roughly temperature-independent. Then, in the second term on the RHS of equation (14), the q_e term is treated as negligible, and the other loss terms, q_r and q_g, are viewed as constants characteristic of a particular absorption chiller. The final approximate formula for COP is then

$$1/\mathrm{COP} = \left[\frac{T_c^{in} - T_e^{out}}{T_e^{out}}\right]\left[\frac{T_g^{in}}{T_g^{in} - T_c^{in}}\right] + \left[\frac{1}{Q_e}\right]\left[\frac{T_g^{in}}{T_g^{in} - T_e^{in}}\right]\left[B_1 - B_2\frac{T_c^{in}}{T_g^{in}}\right] \quad (15)$$

where the constants B_1 and B_2 characterize the irreversibilities of a particular chiller.

5.3. *Model confirmation*

Evidence of confirmation of the functional dependences predicted by equation (15), and of the accuracy in predicting chiller COP values, was presented in ref. [11], where 50 experimental measurements were cited for a nominal 7 kW commercial LiBr–water hot-water-fired absorption chiller [18]. Cooling capacity was varied by roughly a factor of 7 by varying T_c^{in}, T_e^{out} and T_g^{in} within manufacturer-prescribed ranges.

According to equation (15), a plot of

$$\left[\frac{T_g^{in} - T_c^{in}}{T_g^{in}\,\mathrm{COP}} - \frac{T_c^{in} - T_e^{out}}{T_e^{out}}\right]Q_e$$

against T_c^{in}/T_g^{in} should yield a straight line of slope $-B_2$ and extrapolated ordinate intercept B_1—the same straight line at all condenser inlet temperatures. Experimental confirmation is illustrated by Fig. 6(a), where, to within the experimental uncertainty of $\pm 5\%$ in the ordinate values, all 50 data points appear to be well fitted by the simple linear relation predicted (goodness-of-fit $R = 0.993$). With the regression parameters obtained from Fig. 6(a), the experimental COP values are then predicted with an RMS error of 3.85% [see Fig. 6(b)], which is below the experimental uncertainty of $\pm 6.2\%$ [11].

Chiller operating parameters in this case happened to place chiller performance on the linear part of the characteristic curve of Fig. 2 [equation (15)]. Absorption chillers can be driven at sufficiently high cooling rates, however, that non-linearities, due to saturation effects in the generator and absorber as well as finite-rate heat transfer, become noticeable. Even the point of maximum COP (the minimum in the graph of Fig. 2) is experimentally accessible.

To illustrate this point, we cite performance curves

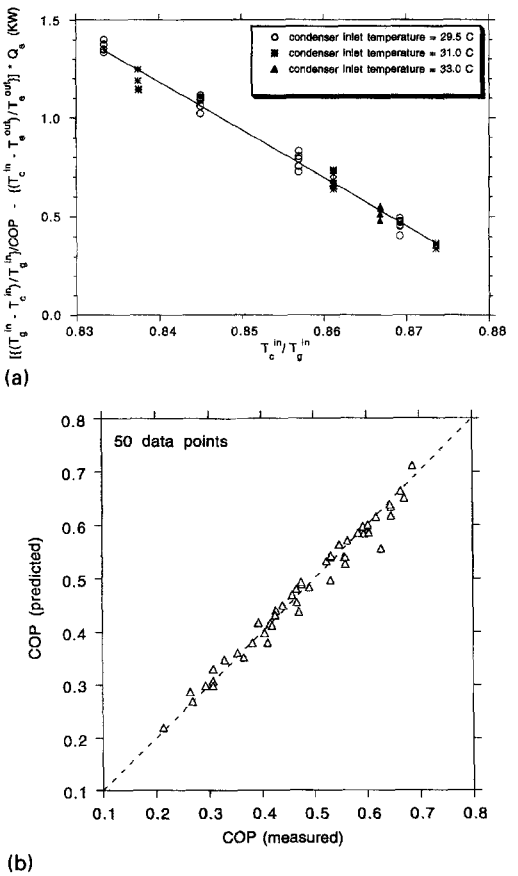

Fig. 6. (a) Check of predicted functional dependence of equation (15) for a nominal 7 kW absorption chiller. To within the (relatively large) experimental uncertainty, all data points collapse to a single straight line. (b) Illustration of accuracy of linear model in predicting absorption chiller COP. Predicted COP is plotted against measured COP for a nominal 7 kW chiller.

(and not individual measurements) for steam- and hot-water-fired commercial absorption chillers as presented in a manufacturer's catalog [5]. One set of curves, presented as relative generator heat input against relative cooling rate, pertains to 23 different chillers that range in size from 355 to 5840 kW. The term 'relative' is used because, for each chiller, both generator heat input and cooling rate are expressed relative to their values at nominal design-load conditions.

Figure 7 presents these curves plotted as $\mathrm{COP}_{\mathrm{design\ load}}/\mathrm{COP}$ against $(\text{cooling rate})_{\mathrm{design\ load}}/(\text{cooling rate})$ at assorted condenser inlet temperatures. Essentially, this is a plot of (constant/COP) vs (constant/cooling rate), where the constants are different for each of the 23 chillers. For relatively low cooling rates, 1/COP is linear in 1/(cooling rate), as per the model prediction. However, at higher cooling rates, these chillers exhibit a maximum COP value,

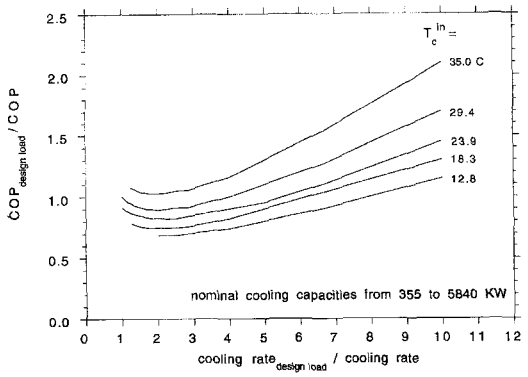

Fig. 7. Characteristic chiller plot for absorption chillers. Note that chiller behavior is predominantly in the linear regime, but may extend beyond the linear region of low cooling rates, through the point of maximum COP.

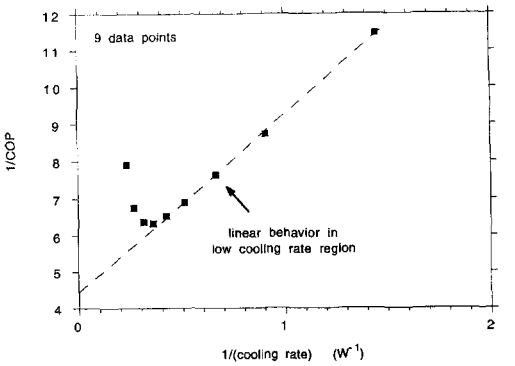

Fig. 8. Characteristic chiller plot for a small thermoacoustic refrigerator.

beyond which there is a narrow region where COP decreases as the cooling rate increases further.

6. THERMOACOUSTIC REFRIGERATORS

In thermoacoustic refrigeration, high-intensity sound waves are used instead of compressors to set up a standing wave in a closed resonator tube filled with inert gases, and in which a stack of plates is inserted with heat exchangers at its ends [19, 20]. The gas is compressed by the acoustic standing wave, warms up, and transfers heat to the stack plates. A heat exchanger rejects part of this heat, and the remaining cooled gas is used to chill the load via the other heat exchanger. There are external irreversibilities such as finite-rate heat transfer at the heat exchangers, and internal irreversibilities, such as fluid friction and imperfect thermal contact between the acoustically oscillating working fluid and the stack plates. The most notable use of the thermoacoustic refrigerator has been as a cryocooler in satellites [20], where using low input power and having large temperature spans (100–200 K) are critical (in contrast, for example, to commercial reciprocating chillers which have far higher input powers and far smaller temperature spans).

The relative contributions of the assorted irreversibilities in thermoacoustic refrigerators can be considerably different from those in commercial chillers. Our purpose here is not to offer a detailed predictive model for the thermoacoustic device, but rather to point out that its performance curve is consistent with the qualitative behavior predicted by our model in Fig. 2, and that the thermoacoustic chiller exhibits a linear region on this curve at cooling rates that are low enough for the COP cooling-rate dependence to be dominated by internal losses. These points are illustrated in Fig. 8, which is a characteristic plot based on data from ref. [20].

7. THERMOELECTRIC REFRIGERATORS

When an electrical current is passed through two dissimilar thermoelectric materials [denoted by A and B in Fig. 1(c), usually metal or semiconductor alloys], one heats up while the other grows colder. Referred to as the Peltier effect, it forms the basis for thermoelectric refrigeration [21, 22]. What may be unique about the thermoelectric cooler is that its performance curve can be measured experimentally over the complete theoretical range, namely, no mechanical or material constraints limit experimentally accessing the full (theoretical) operating range.

Finite-rate heat transfer losses are usually negligible in thermoelectric chillers. Rather, the two dominant irreversibilities are electrical resistivity and heat leak (between the reservoirs, through the thermoelectric chiller). High-efficiency thermoelectric materials inherently possess both a high thermal conductivity and a high electrical conductivity [21, 22]. Electrical resistive losses degrade chiller performance in the high-current, high-cooling-rate limit, and heat leak reduces performance at low currents and low cooling rates.

The cooling capacity Q_e and COP can be expressed in terms of electrical current I by [21, 22]

$$Q_e = \alpha I T_{cold} - K(T_{hot} - T_{cold}) - (I^2 R/2) \quad (16)$$

$$\mathrm{COP} = \frac{\alpha I T_{cold} - K(T_{hot} - T_{cold}) - (I^2 R/2)}{\alpha I (T_{hot} - T_{cold}) + I^2 R} \quad (17)$$

where T_{hot} and T_{cold} are the temperatures of the hot and cold reservoirs, respectively, R is the total electrical resistance of the couple, K is the thermal conductance of the two arms of the couple in parallel, and α is the differential thermoelectric power (differential Seebeck coefficient). Both COP and Q_e exhibit (measurable) maxima, but at different currents.

The characteristic plot of Fig. 2 cannot be drawn in its entirety because the thermoelectric chiller operates normally up to the limits of zero cooling rate and zero COP. An expanded view of the characteristic plot is shown in Fig. 9(a). The linearity of the heat conduction that governs losses at low cooling rates dictates the linear dependence of 1/COP on $1/Q_e$. Figure 9(b) is a plot of COP against cooling rate for the same device, which shows the full range of operating conditions.

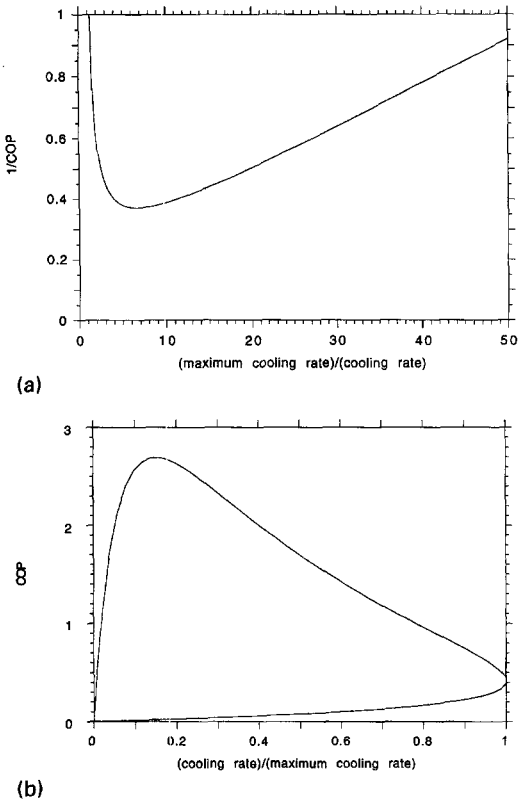

Fig. 9. (a) Characteristic chiller plot for a high-efficiency thermoelectric refrigerator with cold reservoir at 280 K and hot reservoir at 300 K. An expanded view is shown because both COP and cooling rate can be brought to zero in normal operation. (b) Performance characteristics of the thermoelectric refrigerator of Fig. 9(a) plotted so as to show the full operating range.

An interesting contrast between thermoelectric and most common commercial chillers is the region of the characteristic plot where chillers are operated. As noted in Sections 3–5, reciprocating, centrifugal and absorption chillers are operated in the linear regime of Fig. 2, namely, at relatively low cooling rates (or, more properly, where irreversibilities that disfavor slow operation dominate the cooling-rate dependence of chiller COP), usually no higher than those cooling rates at which COP is maximized (the minimum point in Fig. 2).

Thermoelectric chillers, however, are not subject to the same material and mechanical constraints as commercial chillers, are operable over the full range of theoretical (and achievable) cooling rates, and invariably are run between conditions of maximum COP and maximum cooling rate. In the characteristic plot shown in Fig. 9(a), this corresponds to the curve to the left of the minimum point. In fact, there is no practical incentive to operate the thermoelectric chiller at the relatively low cooling rate, linear regime in which most commercial chillers operate. Unlike all other chiller types, finite-rate heat transfer to and from the heat reservoirs is typically not a bottleneck effect under any operating conditions (electrical current values) for thermoelectric chillers. This is part of the reason that the regime of relatively high cooling rates is so readily attainable experimentally.

Since the relatively simple and analytic equations (16) and (17) accurately represent the experimental behavior of thermoelectric refrigerators, there is no need for simplifying models, as was the case for the other chiller types studied here. The thermoelectric refrigerator is offered as an example of an unconventional chiller which exhibits the same primary qualitative features of the characteristic performance curve as do the other classes of chillers modeled here.

8. SUMMARY

Chillers are thermodynamically complex entities for which an accurate, quantitative account of thermodynamic performance has been viewed as requiring detailed, device-specific modeling. Our objective has been to develop a relatively simple thermodynamic model that captures the essential physics of the problem, predicts the correct functional relations among key performance variables, and can be used for quantitative evaluation of system performance and diagnostic studies. The predictive and diagnostic values of the model have been demonstrated with experimental performance data from reciprocating, centrifugal and absorption chillers. The fact that the qualitative trends inherent in the model are also valid for markedly different chiller types has been illustrated with thermoacoustic and thermoelectric refrigerators.

In most, if not all, classes of chillers, irreversibilities will exist that disfavor both high and low cooling rates. Hence, the characteristic chiller plot of 1/COP against 1/(cooling rate) should have the trends shown in Fig. 2. Although chiller behavior should in theory span a broad range of cooling capacities that would confirm the type of curve shown in Fig. 2, in reality, due to mechanical, materials and cost constraints, most chillers are built to operate only along the linear part of this characteristic curve. This has been confirmed from the analysis of many commercial chiller units [9, 11, 15]. This regime of seemingly relatively low cooling rates corresponds to the fact that the dominant contributions to the cooling-rate dependence of commercial chiller COP come from losses that militate against low cooling rates, such as fluid friction, throttling, de-superheating and heat leaks, as opposed to losses due to finite-rate heat transfer.

Subject to a few additional observations about the functional dependence of the particular irreversibility mechanisms on key system variables, we have derived a model that can accurately account for the performance curves of reciprocating and centrifugal chillers with a three-parameter model, and for absorption chiller behavior with a two-parameter model. Because the physical basis for the model is clearly formulated, and not based on empirical fits, one can also state the conditions under which the linear approximations will grow inadequate. For com-

mercial chillers, this corresponds to a significant dependence of COP on cooling rate stemming from finite-rate heat transfer. Although in the less common non-linear regime our model possesses too many adjustable parameters to be deemed practical, it does capture the correct trends displayed by real chiller performance data.

The thermodynamic model can be used diagnostically, for example when chiller performance changes over time, and when the manner and degree to which the chiller COP has degraded, along with its dependence on measurable system variables, need to be ascertained. The model is also able to predict chiller performance over the full range of anticipated operating conditions from a number of measurements that is far less than the number currently made and cataloged. A small number of judiciously-selected measurements permit determination of the coefficients with which chiller performance can be predicted accurately. We have confirmed the validity of these exercises with experimental data for a wide range of commercial chillers. As shown for the primary chiller classes, as well as for thermoacoustic and thermoelectric refrigerators, one can view chiller operation in a universal irreversible thermodynamic framework that in principle is applicable to all chillers.

REFERENCES

1. Trane Co., Cold generator reciprocating liquid chillers, 70 to 120 tons water-cooled and condenserless, Catalog CG-DS-4, Publication PL-RF-CG-000-DS-4-690, La Crosse, WI (1990).
2. Toyo Carrier Engineering Co., 30 HKA, HK, HR packaged hermetic reciprocating chillers 50 Hz, 45.4 to 461 KW, 15 to 160 tons, Publication EPD9107-1(S), Tokyo (1991).
3. Trane Co., Air cooled reciprocating liquid chillers, series CGAV 330 KW through 1180 KW, Societe Trane, Publication C47SD603E-0892, Golbey (1992). The specific chiller cited in Figs. 4 and 5 is model CGAV 428.
4. Carrier International Corp., Packaged cooling units (small air-cooled chillers), Models 50DP016-020, Catalog No. 005-013, Syracuse, NY (December 1984).
5. Trane Co., Single stage absorption cold generator: 101 to 1660 tons, Catalog ABS-DS-1, La Crosse, WI (March 1989).
6. Air Conditioning and Refrigeration Institute, ARI Standard 590, Standard for reciprocating water-chilling packages, Arlington, VA (1986).
7. Air Conditioning and Refrigeration Institute, ARI Standard 550, Standard for centrifugal or rotary water-chilling packages, Arlington, VA (1986).
8. Air Conditioning and Refrigeration Institute, ARI Standard 560, Standard for testing absorption chilling packages, Arlington, VA (1982).
9. J. M. Gordon and K. C. Ng, Thermodynamic modeling of reciprocating chillers, *J. Appl. Phys.* **75,** 2769–2774 (1994).
10. I. Cerepnalkovski, *Modern Refrigerating Machines*. Elsevier Science, Amsterdam (1991).
11. J. M. Gordon and K. C. Ng, A general thermodynamic model for absorption chillers: theory and experiment, *Heat Recovery Systems & CHP* **15,** 73–83 (1995).
12. D. J. Leverenz and N. E. Bergan, Development and validation of a reciprocating chiller model for hourly energy analysis programs, *ASHRAE Trans.* **89**(1A) 156–174 (1983). Performance data for 10, 20 and 50 ton chillers are presented.
13. K. C. Ng, T. Y. Bong and H. T. Chua, Macroscopic modeling of water-cooled reciprocating chillers, submitted to *Int. J. Refrig.* (1994).
14. K. C. Ng, T. Y. Bong and H. T. Chua, Performance evaluation of centrifugal chillers in an air-conditioning plant with building automation systems (BAS), *J. Power Energy* (in press).
15. J. M. Gordon, K. C. Ng and H. T. Chua, Centrifugal chillers: thermodynamic modeling and a diagnostic case study, submitted to *Int. J. Refrig.* (1994).
16. F. Ziegler, F. Brandl, J. Volkl and G. Alefeld, A cascading two-stage sorption chiller system consisting of a water–zeolite high temperature stage and a water–LiBr low-temperature stage, *Proceedings of the CEC Absorption Heat Pumps Congress*, 20–22 March 1985, Paris, pp. 231–238, Commission of the European Communities, Brussels (1985).
17. P. T. Tsilingiris, Theoretical modelling of a solar air conditioning system for domestic applications, *Energy Conversion Mgmt* **34,** 523–531 (1993).
18. Yazaki Resources Co. Ltd., Installation and service manual, WFC-600 Model, Yazaki Corp., Shizuoka-ken. Preliminary results and a full description of our experimental procedures were published in: B. Heling, T. Y. Bong and K. C. Ng, Performance of a lithium bromide–water absorption chiller, *Proceedings of the National Committee on World Energy Council Seminar*, Singapore, November 1992.
19. G. W. Swift, Thermoacoustic engines, *J. Acoust. Soc. Am.* **84,** 1145–1180 (1988).
20. S. L. Garrett and T. J. Hofler, Thermoacoustic refrigeration, *ASHRAE J.* **34**(12), 28–36 (December 1992).
21. A. F. Ioffe, *Semiconductor Thermoelements and Thermoelectric Cooling*. Infosearch, London (1957).
22. H. J. Goldsmid, *Applications of Thermoelectricity*. Methuen, New York (1960).